104 (2025) 105257

Contents lists available at ScienceDirect

Poultry Science

journal homepage: www.elsevier.com/locate/psj

Naringenin as a phytogenic adjuvant systematically enhances the protective efficacy of H9N2 inactivated vaccine through coordinated innate-adaptive immune priming in chickens

Lina Jiao [a,b], Zuchen Song [a,b], Yantong Zhou [a,b], Tianyu Zhu [a,b], Ruihong Yu [a,b], Zheng Wang [a,b], Yawei Qiu [b], Jinfeng Miao [b], Shun Zhang [c], Zhenguang Liu [a,b], Deyun Wang [a,b,*]

[a] Institute of Traditional Chinese Veterinary Medicine, College of Veterinary Medicine, Nanjing Agricultural University, Nanjing 210095, PR China
[b] MOE Joint International Research Laboratory of Animal Health and Food Safety, College of Veterinary Medicine, Nanjing Agricultural University, Nanjing 210095, PR China
[c] Guoke Ningbo Life Science and Health Industry Research Institute, Ningbo 315000, Zhejiang, PR China

ARTICLE INFO

Keywords:
Naringenin
H9N2
Vaccine adjuvant
Viral challenge

ABSTRACT

Although inactivated vaccines remain the primary strategy for preventing and controlling avian influenza virus, they fail to induce durable and systemic immune protection. Adjuvants are crucial for enhancing antigen immunogenicity and improving immune responses. In this study, we evaluated the adjuvant activity of naringenin (**Nar**) for H9N2 inactivated vaccine by detecting humoral immunity, cellular immunity, and viral challenge. The results demonstrated that Nar/H9N2 co-administration significantly increased IgG levels and hemagglutination inhibition (**HI**) titers. Nar/H9N2 promoted the formation of high-affinity antibodies by upregulating the expression of genes associated with B cell activation and germinal centers (**GCs**) formation, thus facilitating humoral immune responses. Concurrently, Nar/H9N2 vaccine enhanced T cell proliferation, $CD4^+$and $CD8^+$ *T* cell differentiation, and the expression of Th1/Th2 cytokines, thereby promoting cellular immunity. Crucially, compared to the inactivated H9N2 vaccine alone, viral challenge experiments confirmed that Nar-adjuvanted immunization confers superior protection, markedly reducing viral shedding and minimizing damage to the trachea and lungs. These findings elucidate the capacity of naringenin to synchronize multifaceted immune activation through GCs optimization and T-cell modulation, establishing Nar as a viable candidate for poultry vaccine adjuvants.

Introduction

Since its initial isolation in Guangdong Province, China (Guo et al., 2003; Sun and Liu, 2015; Sun, et al., 2010), the H9N2 avian influenza virus (**AIV**) has become one of the predominant low-pathogenic avian influenza (**LPAI**) subtypes in Chinese avian populations (Gu, et al., 2017; Liu, et al., 2024b), characterized by rapid transmission, low pathogenicity, and minimal mortality (Tan, et al., 2023; Yang, et al., 2023). H9N2 infection typically induces mild respiratory and gastrointestinal symptoms in poultry, and thus, due to its predominantly subclinical presentation, H9N2 has been excluded from national mandatory vaccination programs (Li, et al., 2014). However, H9N2 infection imposes significant economic burdens on the poultry industry by reducing poultry weight gain (12-26 % in broilers) (Bin Aslam, et al., 2024) and egg production efficiency (15-38 % in layers) (Bonfante, et al., 2018; Dharmayanti, et al., 2020; Shin, et al., 2016; Sun and Liu, 2015). Notably, H9N2 exhibits substantial potential for cross-species transmission to mammals, including pigs (Xu, et al., 2004; Yu, et al., 2008), dogs (Borland, et al., 2020; Zhang, et al., 2013), minks (Xue, et al., 2018; Yong-feng, et al., 2017), and humans (Tan, Zeng, Xie, Li, Liu, Yang, Yang and Wang, 2023). Genomic surveillance reveals that H9N2 viruses continuously undergo antigenic drift and genetic reassortment events (Sun, et al., 2012; Zhu, et al., 2022). These viruses donate internal genes to novel highly pathogenic avian influenza (HPAI) strains (e.g., H5N1 clade 2.3.4.4b and H7N9 fifth-wave variants)(Castro-Sanguinetti, et al., 2024; Liu, et al., 2024a), elevating zoonotic risk. These challenges

* Correspondence author at. Institute of Traditional Chinese Veteri-nary Medicine, College of Veterinary Medicine, Nanjing Agricultural University, Nanjing 210095, PR China.
E-mail address: dywang@njau.edu.cn (D. Wang).

https://doi.org/10.1016/j.psj.2025.105257
Received 17 March 2025; Accepted 2 May 2025
Available online 2 May 2025

underscore the urgent need for innovative immunization strategies, particularly adjuvanted vaccines, to enhance protective immunity and mitigate the risk of zoonotic spillover.

Vaccination serves as the cornerstone prophylactic measure against H9N2 AIV, complementing active biosecurity surveillance systems (Sagong, et al., 2023). Current vaccine preparations against H9N2 AIV encompass inactivated whole-virus vaccines (Dong, et al., 2022; Liu, et al., 2023b), live attenuated strains (Choi, et al., 2015; Wang, et al., 2018), recombinant subunit proteins (Li, et al., 2024), virus-like particle (**VLP**) platforms (Li, et al., 2017; Xu, et al., 2020), and nucleic acid-based vaccines including both DNA and mRNA platforms (Xu, et al., 2023; Zhang, et al., 2023, 2024). While inactivated formulations remain predominant in field applications due to their established safety profiles and manufacturing feasibility, suboptimal immunogenicity frequently necessitates elevated antigen concentrations and repeated adjuvanted boosters (Xie, et al., 2025). Live attenuated vaccines, although capable of eliciting superior immunogenicity, carry risks of virulence reversion and environmental shedding (Subbarao, 2021). Meanwhile, recombinant, VLP-based candidates, and nucleic acid vaccines demonstrate high safety and antigenic specificity but face constraints in industrial - scale bioprocessing and barriers to economic viability (Qian, et al., 2020).

Adjuvant-mediated immunomodulation presents a pivotal avenue for surmounting the limitations of existing vaccines by enhancing immunogenicity and the durability of the immune response (Shichinohe and Watanabe, 2023; Tregoning, et al., 2018). Conventional adjuvant systems, such as oil-in-water emulsions (Camilloni, et al., 2015), aluminum-based formulations (Marrack, et al., 2009), and CpG oligonucleotides (Pan, et al., 2023), have been proven to be efficacious in elevating H9N2-specific antibody titers and cellular immune responses. Nevertheless, the implementation of these adjuvants is often encumbered by off-target immunostimulation, manifested by injection-site granuloma formation, Th2 polarization, or systemic cytokine storm that undermine both safety profiles and protective longevity (Bernstein, et al., 2008; Feltelius, et al., 2015; Sturkenboom, 2015). To overcome the limitations of traditional adjuvants, significant efforts have been devoted to the development of novel adjuvant platforms. Emerging systems, including chitosan-based nanocomposites (Jia, et al., 2025; Lai, et al., 2025), modified aluminum salts (Jin, et al., 2025; Liu, et al., 2023a), and molecular pattern-based immunostimulators, have demonstrated potent immunoenhancing effects in H9N2 and other influenza vaccine models. However, many synthetic or nanoparticle-based adjuvants continue to face translational challenges related to cost, formulation stability, and biocompatibility. Consequently, plant-derived adjuvants with intrinsic immunomodulatory properties have garnered increasing attention as promising alternatives for enhancing vaccine efficacy while ensuring safety and biocompatibility.

Naringenin (**Nar**) is a flavonoid compound primarily detected in citrus fruits, tomatoes, and traditional herbs such as *citrus aurantium L.* and *Dendrobium nobile* (Zhao, et al., 2021). Naringenin demonstrates multimodal pharmacological activities encompassing potent antioxidant, anti-inflammatory, antimicrobial, anticancer, and immunomodulatory effects (Rehman, et al., 2018; Singh, et al., 2023). Notably, naringenin has demonstrated broad antiviral potential, with efficacy against viruses such as hepatitis C virus (**HCV**), herpes simplex virus (**HSV**), dengue virus, severe acute respiratory syndrome coronavirus 2 (**SARS-CoV-2**), and influenza viruses (Morimoto, et al., 2022; Ninfali, et al., 2020). More importantly, the plant-derived naringenin exhibits excellent biosafety and potent immunomodulatory properties compared to conventional aluminum-based adjuvants. Despite these pleiotropic properties, the application of naringenin as an immunostimulatory adjuvant—specifically its capacity to enhance H9N2 influenza vaccine immunogenicity while maintaining biocompatibility—remains conspicuously unexplored, particularly regarding its mechanistic basis and translational potential in poultry vaccinology.

In this study, we conducted a systematic evaluation of Nar as an adjuvant for the H9N2 inactivated vaccine. Our findings demonstrate that the administration of Nar/H9N2 synergistically amplifies both humoral and cellular immune responses elicited by the H9N2 vaccine, promoting a robust systemic immune activation without triggering immunopathology reactions. Moreover, our results indicate that Nar/H9N2 vaccination confers effective protection against influenza virus challenge under cold stress conditions, leading to a significant reduction in viral load within the trachea and lungs while mitigating virus-induced pulmonary and tracheal damage. Collectively, these findings spotlight Nar as a phytogenic adjuvant candidate that strikes a balance between immunopotentiation and biocompatibility, providing new insights for the development of plant-derived adjuvants against avian influenza threats.

Materials and methods

Preparation of H9N2 antigen

The H9N2 AIV strain (AV1563, National Veterinary Microbiology Center, Beijing, China) was propagated in 9-day-old specific-pathogen-free (**SPF**) chicken embryos (Nanjing Tegeili Poultry Farm). Allantoic fluid was harvested to obtain H9N2 virus, and the viral titer was determined by calculating the 50 % embryo infectious dose ($\mathbf{EID_{50}}$). The virus was then inactivated by adding 0.05 % formaldehyde (4°C, 48 hours) to yield the inactivated H9N2 antigen. The hemagglutination assay (**HA**) was performed using chicken red blood cells (Senbeijia Biotech Co., Ltd) to assess the viral titer of the inactivated antigen.

Preparation of vaccine adjuvant

The naringenin-adjuvanted H9N2 inactivated vaccine (**Nar/H9N2**): DMSO (50 μL, 5 %), PEG400 (50 μL, 5 %), and PBS (400 μL) were sequentially added to 20 mg of naringenin (MedChemExpress Co., Ltd), followed by sonication to ensure complete dissolution of naringenin. The mixture was mixed 1:1 (v/v) with inactivated H9N2 antigen (HI titer 2^8) to obtain Nar/H9N2 vaccine. Naringenin had a final concentration of 20 mg/mL.

The non-adjuvanted H9N2 inactivated vaccine (**H9N2**): The H9N2 vaccine was prepared by identical methodology, substituting naringenin with equivalent volumes of DMSO-PEG400-PBS vehicle. An equal volume of inactivated H9N2 antigen (HI titer 2^8) was then added to the mixture to obtain H9N2 vaccine.

The aluminum-adjuvanted H9N2 inactivated vaccine (**Alum/H9N2**): Alum adjuvant (Biodragon Technology Co., Ltd) was diluted with PBS and mixed with an equal volume of inactivated H9N2 antigen (HI titer 2^8) to obtain Alum/H9N2 vaccine. Aluminum hydroxide had a final concentration of 1 mg/mL.

PBS group: For the PBS control group, DMSO, PEG400, and PBS were mixed in the same proportion as used in the vaccine formulations. Then, the antigen was replaced with an equal volume of PBS to serve as a negative control.

Immunization protocol

A total of 180 one-day-old female brown broiler chickens (Nanjing Tegeili Poultry Farm) were housed at the Experimental Animal Facility Center of Nanjing Agricultural University. During the initial rearing phase, chickens were maintained at 32°C for 3 days, and then the temperature was gradually decreased by 0.5°C per day. After two weeks, the room temperature was maintained at about 24°C. The chickens were provided with a regular 12-hour light cycle, and had unrestricted access to sufficient feed and drinking water. Once maternal antibodies were undetectable, chickens were randomly assigned into 4 groups: PBS group, H9N2 group, Nar/H9N2 group, and Alum/H9N2 group, with 30 chickens in per group. Each chick was immunized via intramuscular injection with 500 μL of the respective vaccine formulation. A booster

immunization was administered on day 14 post-primary immunization.

All experimental procedures were conducted in accordance with the guidelines outlined in the Guide for the Care and Use of Laboratory Animals by the National Research Council and were reviewed and approved by the Institutional Animal Care and Use Committee (**IACUC**) of Nanjing Agricultural University (NJAU.No20231120171).

Antibody and hemagglutination inhibition assay

On days 21, 28, and 35 after the initial immunization, 6 chickens were randomly selected from each group to collect blood samples for evaluating antibody response.

To assess H9N2-specific IgG antibody levels, an enzyme-linked immunosorbent assay (**ELISA**) was carried out in the following manner: Inactivated H9N2 antigen was coated onto 96-well plates and incubated for 12 hours (4°C). The plates were then incubated with 5 % skim milk for 2 hours at 37°C to perform the blocking step. The serum samples that have been diluted were added and incubated for 1 hour at 37°C, followed by incubation with anti-chicken IgG secondary antibody (Beijing Boaosen Biotech Co., Ltd) for another hour at 37°C. At each interval between steps, PBST was used to wash the plates three times. Finally, a substrate solution (Solarbio Science & Technology Co., Ltd) was added for color development, followed by a stop solution, and the microplate reader was used to measure OD_{450}.

To determine hemagglutination inhibition (**HI**) antibody titers, serum samples were heat-inactivated at 56°C for 30 minutes. The inactivated serum was serially two-fold diluted in a 96-well microplate, followed by the addition of an equal volume of inactivated H9N2 antigen (4 HA units) and incubation at 25°C for 30 minutes. Then, 1 % chicken red blood cell suspension was incubated for 30 minutes, and the highest dilution of the serum that entirely prevented hemagglutination was recorded as the HI titer.

Peripheral blood lymphocyte proliferation assay

On day 21 post-primary immunization, 6 chickens were randomly chosen from each group to collect blood samples with anticoagulant tubes. The collected blood was diluted with PBS 1:1 (v/v) and gently added onto the lymphocyte separation medium (Solarbio Science & Technology Co., Ltd). The mixture was centrifuged (2000 rpm, 30 min) and the intermediate lymphocyte layer was carefully collected. The isolated lymphocytes were washed twice with PBS RPMI 1640 and transferred into RPMI 1640 complete medium fortified with 10 % fetal bovine serum (**FBS**, Suzhou Excell Biotechnology Co., Ltd), 1 % penicillin-streptomycin (Yeasen Biotech Co., Ltd), and 5 % inactivated H9N2 antigen. The cell suspension (1×10^6 cells/mL) was plated and incubated for 48 hours (37°C). Lymphocyte proliferation in each group was tested using the Cell Counting Kit-8 (**CCK-8**, Yeasen Biotech Co., Ltd) assay.

Immunofluorescence analysis

On day 21 post-primary immunization, spleens were collected from chickens in each group and fixed in 4 % paraformaldehyde for immunofluorescence histological analysis.

Evaluation of immune organ index

On day 21 post-primary immunization, the body weight of each chicken was recorded, and the thymus, spleen, and bursa of Fabricius were collected and weighed. The immune organ index was calculated using the following formula:

$$\text{Immune organ index (g/kg)} = \text{Organ weight (g)}/\text{Body weight(kg)}$$

PCR analysis

Thymus samples, spleens and peripheral blood samples were collected after the primary immunization. The collected tissues were ground in liquid nitrogen and transferred to centrifuge tubes containing Trizol (Yeasen Biotech Co., Ltd) for total RNA extraction. Subsequently, the extracted RNA underwent reverse transcription and was analyzed using quantitative real - time PCR (**qPCR**). The primer sequences are shown in Table 1.

Safety evaluation

On day 42 post-primary immunization, thymus, spleen, bursa of fabricius, liver, and kidney samples were collected. Each organ was flushed with pre-chilled PBS. Subsequently, the organ was immersed in 4 % paraformaldehyde (**PFA**) for histopathological examination.

Challenge protection experiment

Immunization and challenge protocol. Female chickens were randomly assigned to five groups: PBS group, H9N2 group, Nar/H9N2 group, Alum/H9N2 group, and Blank group, with 12 chickens in each group. The Blank group served as a negative control without immunization or viral challenge. Chickens in the immunization groups received an intramuscular injection of 500 μL of the respective vaccine formulation on days 0 and 14. On day 28 post-primary immunization, all chickens in the immunized groups underwent a 12-hour cold stress exposure before and after viral challenge. Subsequently, each chicken was intranasally inoculated with 0.1 mL of H9N2 virus (10^6 EID_{50}).

Body weight monitoring. Following the viral challenge, body weight was measured and recorded every other day.

Histopathological analysis. On day 4 post-challenge, trachea and lung tissues were collected, and macroscopic changes were recorded. The collected tissues were immersed in 4 % PFA, followed by H&E staining for histopathological examination to assess tracheal and pulmonary lesions.

Viral shedding assessment. On day 4 post-challenge, trachea and lung tissues were harvested, and these tissues were then homogenized (4°C) in PBS supplemented with 2000 U/mL penicillin- streptomycin. The homogenized suspensions were centrifuged (10000 rpm, 10 min), and the supernatants were collected. The supernatants were then subjected to serial 10-fold dilutions and inoculated into 9-day-old SPF chicken embryos (37°C, 48 hours). Allantoic fluid was harvested, and the viral shedding was determined by calculating the EID_{50}.

Statistical analysis

All the data obtained in this test were analyzed and plotted with the software Graphpad prism 10.0, and $P < 0.05$ was set as the significant difference and denoted as follows: $^*p < 0.05$, $^{**}p < 0.01$, $^{***}p < 0.001$. The results were expressed as means ± SEM.

Result and discussion

Naringenin enhances the antibody response of H9N2 vaccine

Antibody levels serve as a key indicator of the ability of vaccine to elicit antigen-specific immune responses and are directly correlated with the long-term protective efficacy of vaccination. To comprehensively evaluate the immunostimulatory potential of naringenin as an adjuvant for the inactivated H9N2 vaccine, we measured serum H9N2-specific IgG antibody levels on days 21, 28, and 35 following primary immunization (Fig. 1A). The results demonstrated that the Nar/H9N2 group consistently elicited higher IgG antibody levels than that in H9N2 group within 35 days, with levels comparable to or exceeding those observed in the Alum/H9N2 group (Fig. 1B). These findings suggest that Nar, as a

Table 1
The primer sequences.

Gene	Sense strand (5′–3′)	Antisense strand (5′–3′)
CD40	GGGCTCGTGGTGAAGGTGAAAG	GGATCAGCACTGACAGCGATGAG
AID	GCGTAACAAGATGGGTTGCC	GGGTAGGCACGAAGGAAGTC
TGF-β	ACCTCGACACCGACTACTGCTT	ATCCTTGCGGAAGTCGATGT
BCL6	GCAGTTCAGAGCCCACAAAA	GTTCAGACGGGAGGTGTACA
Blimp-1	ACACAGCGGAGAGAGACCAT	GCACAGCTTGCACTGGTAAG
IRF4	GTGTGGGAGAATGACGAGAAG	AAGGAGATGTGATTGGGAAGG
XBP1	GTGCGAGTCTACGGATGTGA	GTGCGAGTCTACGGATGTGA
IFN-γ	ACGACACCATCCTGGACACC	TTTGGCGTTGGCTGTCGTTC
IL-4	GTGCCCACGCTGTGCTTAC	AGGAAACCTCTCCCTGGATGT
IL-6	AAATCCCTCCTCGCCAATCT	CCCTCACGGTCTTCTCCATAAA
IL-1β	CATCACCAACCAACCCGA	ACGAGATGGAAACCAGCAA
CCR7	CCTGCATGGGACGGGAGGGA	GCTCTGCTGGCCGCCGTTAT
IL-10	CGCTGTCACCGCTTCTTCA	TCCCGTTCTCATCCATCTTCTC
TNF-α	CAGCCCTCACATCACCTC	GCTGCCACTCCAGCAATA
β-actin	AAGCCAACAGAGAGAAGATGACACA	TACAGATCCTTACGGATATCCACAT

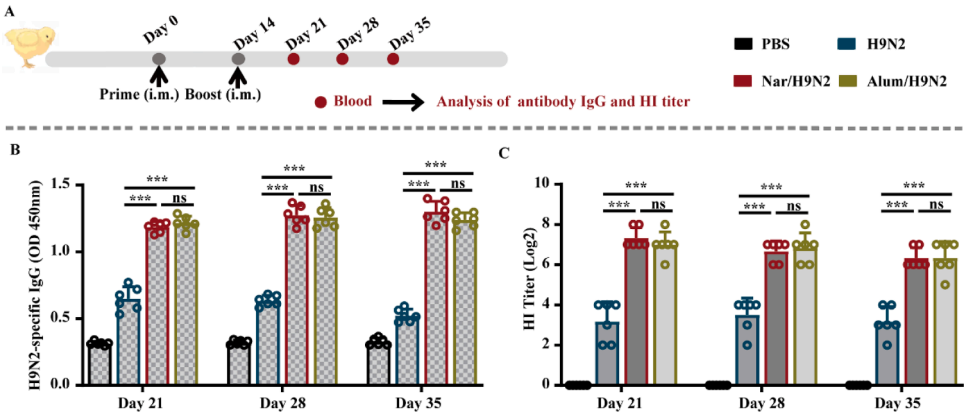

Fig. 1. Naringenin enhances the antibody response of H9N2 vaccine. (A) Schedule of H9N2 immunization program and analysis of antibody. Blood samples were collected on days 21, 28, and 35 post-immunizations, and serum was isolated to assess H9N2-specific IgG antibody levels (B) and HI titers (C). Dates are shown as the mean ± SEM; $n = 6$ independent experiments (*** $p < 0.001$, and ns = no significant differences between groups).

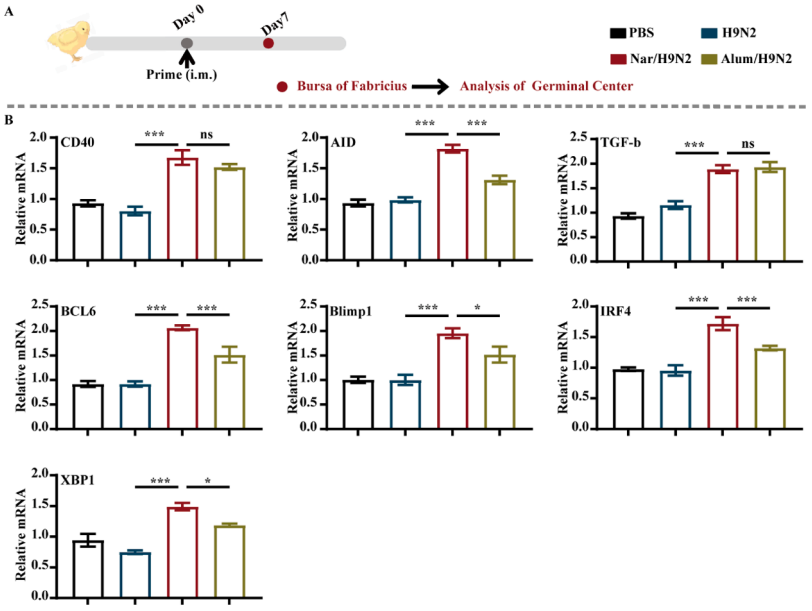

Fig. 2. Naringenin promotes the expression of genes related to germinal centers. (A) Schedule of the H9N2 immunization program and analysis of GCs formation. (B) On day 7 post-immunization, bursae of fabricius were collected from each group to assess the mRNA expression levels of GCs, including CD40, AID, TGF-β, BCL6, Blimp-1, IRF4, and XBP1. Dates are shown as the mean ± SEM; $n = 6$ independent experiments (* $p < 0.05$, *** $p < 0.001$, and ns = no significant differences between groups).

natural flavonoid compound, effectively enhances vaccine-induced antibody production by accelerating the initiation and amplifying the magnitude of the humoral immune response.

IgG antibody quantification primarily assesses the capacity of vaccine to induce specific humoral immunity, whereas HI titers specifically measure functional antibodies targeting viral HA, which is the gold-standard correlate of influenza vaccine efficacy (Heeringa, et al., 2020). A protective HI threshold (≥ 4 $\log_2$) reflects antibody-mediated blockade of HA-receptor binding, a critical determinant of viral neutralization and transmission suppression (Roubidoux, et al., 2021; Zhou, et al., 2024). In this study, the Nar/H9N2 group significantly enhanced HI titers within 35 days (Fig. 1C), which confirms that naringenin effectively promotes the generation of protective antibodies.

Collectively, these findings underscore naringenin as a promising natural adjuvant candidate for the H9N2 inactivated vaccine. By facilitating and potentiating the humoral immune response, naringenin not only enhances IgG antibody titers but also improves antibody functionality and neutralization capacity.

Naringenin promotes the expression of genes related to germinal centers

Following vaccination, germinal centers (**GCs**) constitute a pivotal phase in generating an effective humoral immune response, determining the magnitude and affinity of antibodies (Bhagchandani, et, al.; Viant, et al., 2020). Given the observed enhancement of H9N2-specific IgG and HI titers by Nar, its immunomodulatory impact on GCs dynamics was systematically interrogated (Fig. 2A). During the production of antibody, T follicular helper (**Tfh**) cells orchestrate B cell activation through CD40-CD40L costimulatory interactions, initiating clonal expansion and affinity maturation (Luo, et al., 2018; Watanabe, et al., 2017). This priming enables activated B cells to undergo GCs reactions mediated by activation-induced cytidine deaminase (**AID**), transforming growth factor β (**TGF-β**), and B-cell lymphoma 6 (**BCL6**) transcriptional regulation, which were essential for somatic hypermutation and plasma cell differentiation (Hu and Zhao, 2016; Sun, et al., 2021). Notably, the H9N2 inactivated vaccine failed to upregulate these GCs-associated genes, reflecting its limited capacity to initiate GCs reactions. In contrast, Nar/H9N2 vaccine demonstrated potent upregulation of CD40, AID, TGF-β, and BCL6 expression (Fig. 2B), outperforming Alum/H9N2 group, suggesting that Nar/H9N2 vaccine exerts a beneficial influence on the formation of GCs and the generation of functional antibodies, contributing to a more robust and effective immune response.

Furthermore, during the late stages of the GCs response, the terminal differentiation of B cells into antibody-secreting plasma cells or memory B cells is governed by a transcriptional regulatory axis involving BCL6 (Shehata, et al., 2024), B-lymphocyte induced maturation protein-1 (**Blimp-1**) (Angelin-Duclos, et al., 2000), interferon regulatory factor 4 (**IRF4**) (Bollig, et al., 2012; Ochiai, et al., 2013), and X-box binding protein 1 (**XBP1**) (Rau, et al., 2009). Differentiated plasma cells migrate to the bone marrow to establish sustained antibody production, while memory B cells retain antigenic specificity for rapid recall (Amanna and Slifka, 2010; Cancro and Tomayko, 2021). Compared with the PBS group, the H9N2 inactivated vaccine failed to enhance the mRNA expression of BCL6, Blimp-1, IRF4, and XBP1, indicating a limited ability of the H9N2 inactivated vaccine to drive B cell differentiation into effector cells. Crucially, Blimp-1, IRF4, and XBP1 levels in the Nar/H9N2 group were significantly higher than those in the H9N2 and Alum/H9N2 groups (Fig. 2B), demonstrating the superior capacity of Nar to drive B cell terminal differentiation. Collectively, these findings underscore the superior capacity of the Nar/H9N2 vaccine to potentiate GC-associated immunity compared to the conventional alum adjuvant. Nar/H9N2 orchestrates B cell activation, promotes the generation of high-affinity antibodies, and enhances the differentiation of both plasma cells and memory B cells, thereby improving both the durability and overall efficacy of the H9N2 inactivated vaccine.

Naringenin upregulates the cellular immune response of H9N2 vaccine

Cell-mediated immunity is a critical determinant of vaccine efficacy. Following vaccination, lymphocyte proliferation and activation serve as fundamental processes for initiating cellular immunity (Hivroz and Saitakis, 2016). Moreover, upon antigen restimulation, lymphocyte proliferation not only reflects the degree of adaptive immune activation but also indicates the establishment and recall of immune memory (Santosa and Sun, 2023). To assess the capacity of Nar/H9N2 to potentiate cellular immunity, peripheral blood mononuclear cells (**PBMCs**) were isolated at 21 days post-immunization and subjected to ex vivo H9N2 antigen recall challenge (Fig. 3A). The PBMCs proliferation index in the Nar/H9N2 group was higher compared to the PBS, and H9N2 (Fig. 3B). It is well established that aluminum-based adjuvants primarily elicit humoral immune responses but have limited capacity to induce cellular immunity. Our results demonstrate that Nar/H9N2 vaccine compensates for this limitation of Alum/H9N2 vaccine by significantly enhancing PBMCs proliferation (Fig. 3B), thereby promoting cellular immune activation.

As the principal secondary lymphoid organ coordinating peripheral T cell priming, the spleen provides critical insights into vaccine-induced cellular immunity, with splenic $CD4^+$ and $CD8^+$ T lymphocyte populations serving as quantitative metrics of the dynamic response of immune system to vaccination (Arsenio, 2020; Pereira, et al., 2024). Despite its widespread use, alum exhibits intrinsic limitations in eliciting robust cellular immunity especially in priming of $CD8^+$ T cells. Immunofluorescence analysis of the spleen revealed that the H9N2 inactivated vaccine elicited a slight $CD4^+$ T cell expansion. Compared to the H9N2 group, the Alum/H9N2 group exhibited a significant increase in $CD4^+$ T cells but failed to substantially enhance the proportion of $CD8^+$ T cells, indicating the limited capacity of aluminum-based adjuvants to elicit $CD8^+$ T cell-mediated cellular immunity. Strikingly, the Nar/H9N2 group demonstrated significantly higher fluorescence intensity for both $CD4^+$ and $CD8^+$ T cells compared to the H9N2 and Alum/H9N2 groups (Fig. 3C-F), indicating that the Nar/H9N2 vaccine has a dual activation profile transcending traditional adjuvant limitations, particularly in promoting $CD8^+$ T cell-mediated cellular immunity.

Collectively, these findings indicate that naringenin serves as an effective adjuvant for the H9N2 inactivated vaccine, overcoming the suboptimal cellular immunogenicity inherent to inactivated vaccine and Alum adjuvant. By augmenting PBMCs proliferation and expanding splenic $CD4^+$ and $CD8^+$ T cell populations, naringenin orchestrates coordinated activation of adaptive immunity to achieve superior vaccine-mediated immunological protection.

Naringenin promotes the occurrence of Th1 and Th2 immune responses

Cytokines serve as key mediators of immune responses, and the expression levels of cytokines directly reflect the type, magnitude, and balance of immune response (Cui, et al., 2024; Jiang, et al., 2021). IFN-γ, a hallmark cytokine of Th1-type immunity, is critical for $CD8^+$ T cell-mediated cellular immune responses, playing a central role in combating intracellular pathogens and eliminating infected cells (Seyed and Rafati, 2021). In contrast, Th2-associated cytokines IL-4 and IL-6 primarily promote antibody production through B cell-mediated immune responses (Ansel, et al., 2006; Zeng, et al., 2024). To evaluate the immunomodulatory effects of naringenin, we analyzed mRNA expression levels of key cytokines in the spleen and PBMCs on day 21 post-primary immunization (Fig. 4A). Compared to the H9N2 and Alum/H9N2 groups, the Nar/H9N2 group upregulated the expression of IFN-γ (Fig. 4B and 4C), indicative of enhanced Th1-polarized cellular immunity and cytotoxic $CD8^+$ T cell activation. Concomitantly, IL-4 and IL-6 expression levels in the Nar/H9N2 group were significantly higher than those in the H9N2 group, with expression levels paralleling or exceeding the Alum/H9N2 group (Fig. 4B and 4C). This balanced cytokine induction profile reveals the unique capacity of naringenin to

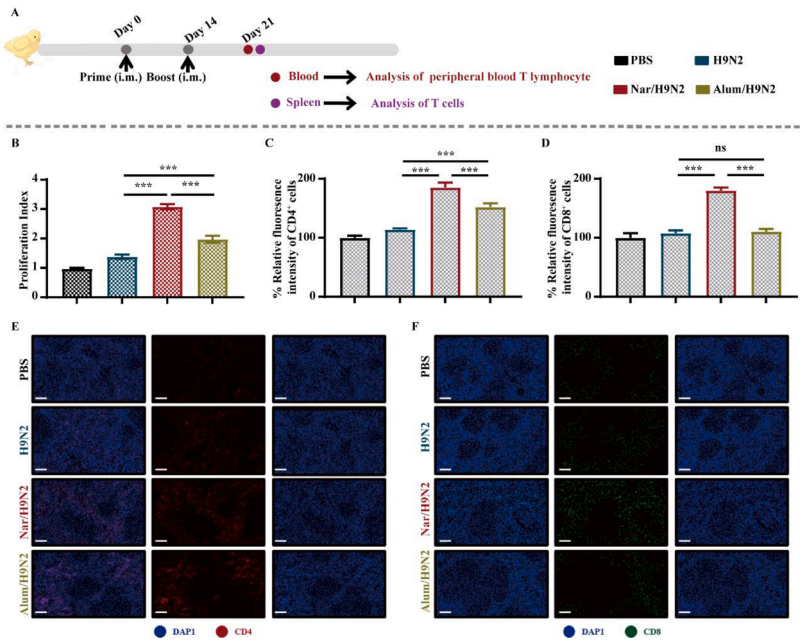

Fig. 3. Naringenin upregulates the cellular immune response of H9N2 vaccine (A) Schedule of H9N2 immunization program and analysis of cellular immunity. (B) On day 21 post-primary immunization, PBMCs were isolated and restimulated with H9N2 antigen in vitro for 48 hours. Lymphocyte proliferation was assessed using the CCK-8 assay. Dates are shown as the mean ± SEM; $n = 6$ independent experiments (*** $p < 0.001$). (C–F) On day 21 post-immunization, spleens were collected for immunofluorescence staining to analyze $CD4^+$ T cells (E) and $CD8^+$ T cells (F). Fluorescence intensity for $CD4^+$ T cells (C) and $CD8^+$ T cells (D) was quantified using ImageJ software. Scale bar = 200 μm. Dates are shown as the mean ± SEM; $n = 3$ independent experiments (*** $p < 0.001$, and ns = no significant differences between groups).

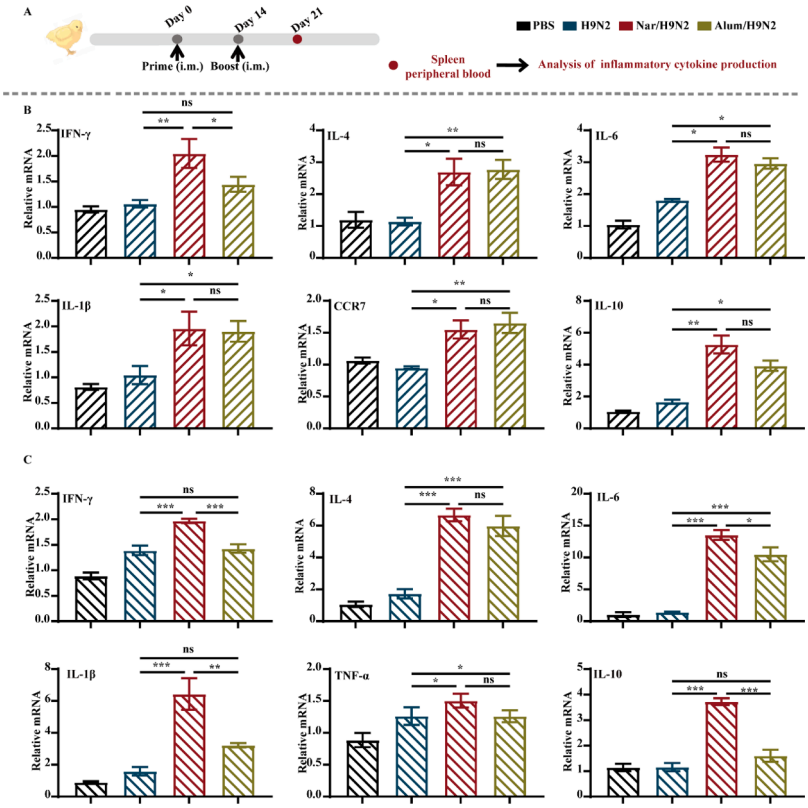

Fig. 4. Naringenin enhances both Th1- and Th2-mediated immune responses. (A) Schematic representation of the H9N2 immunization protocol and cytokine analysis. (B) On day 21 post-immunization, spleens were collected to assess the mRNA expression levels of cytokines, including IFN-γ, IL-4, IL-6, IL-1β, CCR7, and IL-10. (C) On day 21 post-immunization, PBLs were collected and restimulated in vitro for 48 hours, followed by the analysis of cytokine mRNA expression levels, including IFN-γ, IL-4, IL-6, IL-1β, TNF-α, and IL-10. Dates are shown as the mean ± SEM; $n = 6$ independent experiments (* $p < 0.05$, ** $p < 0.01$, and *** $p < 0.001$, and ns = no significant differences between groups).

concomitantly potentiate IFN-γ-driven Th1-type cellular immunity and IL-4/IL-6-mediated Th2-type humoral immunity, achieving coordinated immune programming unattainable with conventional adjuvant systems.

In addition, IL-1β and TNF-α, as prototypical pro-inflammatory cytokines, are essential for inflammatory responses and immune activation (Guo, et al., 2016; Mujal, et al., 2025; Trevejo, et al., 2001). CCR7, a chemokine receptor associated with lymphocyte migration and homing, exerts a beneficial influence on immune priming and memory formation (Comerford, et al., 2013). The Nar/H9N2 group significantly upregulated the expression levels of IL-1β, TNF-α, and CCR7 in both the spleen and PBMCs, highlighting the ability of naringenin to enhance immune activation. More importantly, Nar/H9N2 vaccine markedly upregulated the expression of anti-inflammatory cytokine (IL-10), suggesting that naringenin not only enhances immune responses but also maintains immune homeostasis, reducing the risk of immunopathology (Moore, et al., 2001; Saxton, et al., 2021).

Collectively, these findings emphasize the balanced ability of naringenin in immune activation and homeostatic regulation, effectively mitigating vaccine-associated immunopathology risks while maintaining antigen-responsive immune activation.

Naringenin promotes the development of immune organs

The indices of primary lymphoid tissues (thymus, bursa of fabricius) and secondary lymphoid organs (spleen) can provide valuable insights into the activation of immune responses(Ashby and Hogquist, 2024; Ko, et al., 2018; Lewis, et al., 2019). To evaluate the impact of Nar/H9N2 vaccination on overall immune function, immune organ indices were assessed on day 21 post-primary immunization (Fig. 5A). Compared with the H9N2 group, the Nar/H9N2 group exhibited a significant increase in spleen indices, while showing an upward trend in the thymus and bursa indices (Fig. 5B-D). These findings suggest that naringenin enhances the immunogenicity of the inactivated H9N2 vaccine by promoting both T and B cell development, thereby systematically strengthening the vaccine-induced immune response.

Biological safety of naringenin as adjuvant for H9N2 Vaccine

Biosafety is a critical consideration in the design and application of vaccine adjuvants. To assess the biosafety of Nar/H9N2 vaccine, histopathological analysis was performed on the spleen, thymus, Bursa of fabricius, liver, and kidney on day 42 post-primary immunization (Fig. 6A). H&E staining revealed that the organ structures in the Nar/H9N2 group remained intact, with no observable pathological abnormalities, suggesting that naringenin demonstrates a promising biosafety characteristic as an adjuvant for the H9N2 vaccine.

Naringenin enhances the protective efficacy of H9N2 vaccine

Viral challenge experiments serve as the gold standard for evaluating the protective efficacy of vaccines (Yang, et al., 2017). The protective efficacy of Nar/H9N2 vaccination was evaluated by conducting a viral challenge under controlled hypothermic conditions, simulating natural environmental stressors. To minimize interference from maternally derived antibodies, chickens were immunized at 28 days of age, which maternal antibody levels had declined to the lowest detectable threshold, and challenged with a low-virulence H9N2 vaccine strain at 28 days post-immunization (at 56 days of age) (Fig. 7A). Unvaccinated and unchallenged chickens served as the Blank group. Following the challenge, chickens in the PBS and H9N2 group exhibited growth retardation versus pre-infection baselines, suggesting that viral infection negatively impacted growth performance. In contrast, the Nar/H9N2 group maintained steady weight gain trajectories (Fig. 7B) and outperformed the Alum/H9N2 group in growth preservation, indicating that Nar/H9N2 vaccination contributed to mitigating the adverse effects of viral infection on growth performance.

On day 4 post-challenge, trachea and lung tissues were collected for viral shedding analysis (Wu, et al., 2024). The positive of the virus was confirmed in the PBS and H9N2 groups, with average viral titers of 7.56 $\log_{10}$ EID_{50}/mL and 5.7 $\log_{10}$ EID_{50}/mL in the trachea and lungs of the PBS group, respectively. Similarly, in the H9N2 group, viral titers were 4.06 $\log_{10}$ EID_{50}/mL and 3.25 $\log_{10}$ EID_{50}/mL in the trachea and lungs, respectively. In contrast, viral titers in the Alum/H9N2 and Nar/H9N2 groups were below the detection threshold (Fig. 7C and 7D), indicating that Nar/H9N2 vaccination significantly inhibited viral shedding, thereby enhancing vaccine-mediated protection.

To further evaluate vaccine-mediated protection, macroscopic morphological and histopathological analyses of the trachea and lungs were conducted (Yan, et al., 2024). Macroscopic morphological analysis revealed that no apparent pathological changes were observed in the trachea across all groups. However, H&E staining revealed severe pathological damage in the tracheal mucosal layer of the PBS and H9N2 groups (Fig. 7E), characterized by epithelial detachment (red arrows), mucosal edema (yellow arrows), and infiltration of blood and inflammatory cells (green circles). In contrast, the tracheal structure remained intact in the Alum/H9N2 and Nar/H9N2 groups, showing no significant pathological abnormalities compared to the Blank group. Meanwhile, multifocal necrosis (blue arrows) was observed in the lung tissues of PBS and H9N2 groups, with H&E visualization demonstrating extensive inflammatory exudates (yellow arrows), infiltration of inflammatory cells (red arrows), and alveolar collapse (black arrows). Conversely, no significant pathological alterations were observed in the lung tissues of the Alum/H9N2 and Nar/H9N2 groups, further confirming the protective effects of Nar/H9N2 vaccination against H9N2-induced pulmonary damage.

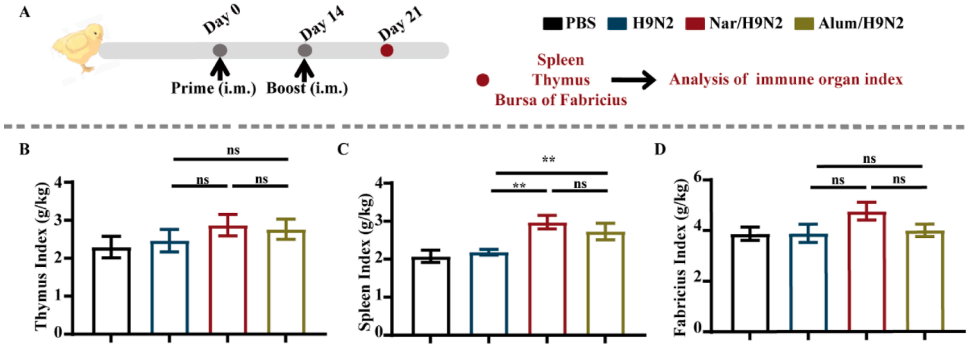

Fig. 5. Naringenin promotes the development of immune organs. (A) Schedule of H9N2 immunization program and analysis of immune organ index. Evaluation of thymus index (B), spleen index (C), and bursa of fabricius index (D) on day 21 post-primary immunization. Dates are shown as the mean ± SEM; $n = 6$ independent experiments (**$p < 0.01$, and ns = no significant differences between groups).

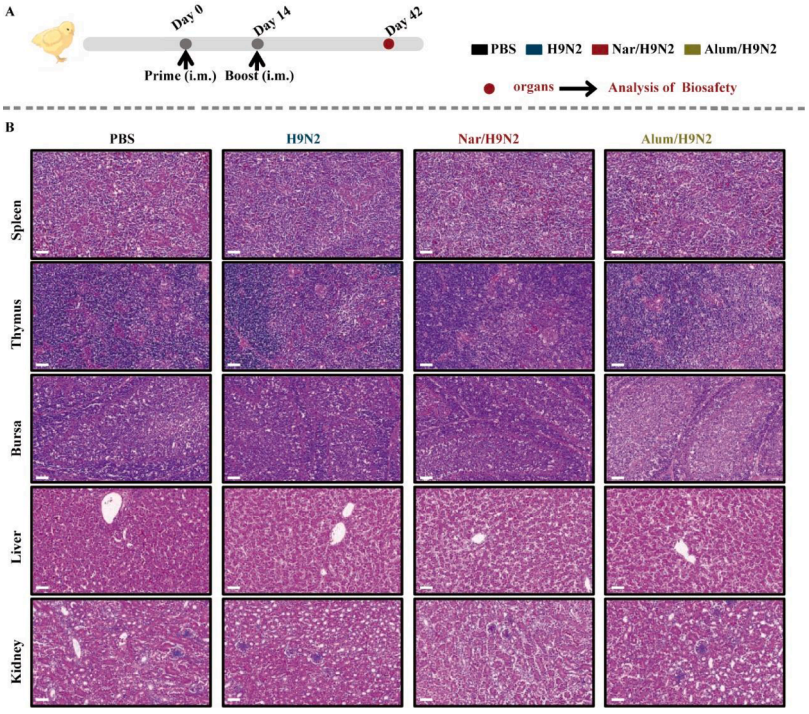

Fig. 6. Biological safety of naringenin as adjuvant for H9N2 Vaccine. (A) Schematic representation of the H9N2 immunization protocol and biosafety analysis. (B) Histopathological examination of the spleen, thymus, bursa of Fabricius, liver, and kidney collected on day 42 post-immunization using H&E staining. Scale bar = 50 μm.

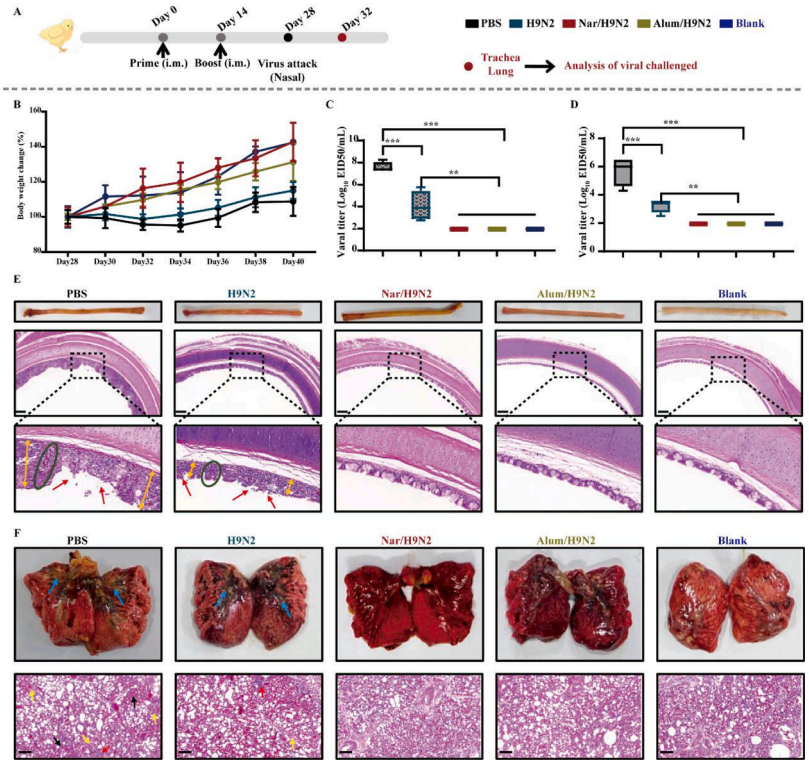

Fig. 7. Naringenin enhances the protective efficacy of H9N2 vaccine. (A) Schematic representation of the H9N2 immunization protocol and viral challenge experiment. (B) Changes in body weight were monitored following viral challenge. On day 4 post-challenge, trachea and lung tissues were collected, homogenized, and inoculated into 9-day-old SPF chicken embryos. Viral shedding of trachea (C) and lung (D) were assessed by EID_{50} after 48 hours of incubation. Macroscopic morphological and H&E histopathological analysis of tracheal (E, scale bar = 200 μm) and lung (F, scale bar = 50 μm) tissues to assess pathological changes. Dates are shown as the mean ± SEM; $n \geq 4$ independent experiments (** $p < 0.01$, and *** $p < 0.001$).

These findings collectively demonstrate that naringenin significantly enhances the immune protection of the H9N2 vaccine, effectively mitigating the negative impact of viral challenge on growth performance and preventing pathological damage to the respiratory organs.

Conclusion

In summary, our study demonstrates that naringenin significantly enhances IgG levels and HI titers induced by the inactivated H9N2 vaccine, while promoting germinal centers formation. Nar/H9N2 immunization markedly increases T cell differentiation and induces a balanced Th1/Th2 immune response. Importantly, the viral challenge experiment confirmes the protective efficacy of Nar/H9N2 vaccine, which reduces viral shedding and mitigates tracheal and pulmonary damage. Given its natural origin, immunomodulatory potential, and biosafety, naringenin represents a novel plant-derived adjuvant for avian influenza vaccines.

Ethics approval and consent to participate

All experimental procedures were conducted in accordance with the guidelines outlined in the Guide for the Care and Use of Laboratory Animals by the National Research Council and were reviewed and approved by the Institutional Animal Care and Use Committee (IACUC) of Nanjing Agricultural University (NJAU.No20231120171).

Availability of dae and materials

All data and analysis results of this work are included in this article

Funding

The project was supported by the National Key Research and Development Program (Grant No. 2024YFD1800401), the National Natural Science Foundation of China (Grant No. 32273048), the Fundamental Research Funds for the Central Universities (No. KJYQ2025005), Young Elite Scientists Sponsorship Program by CAST (2022QNRC001).

Author contributions

Conceptualization: Lina Jiao; Methodology: Zuchen Song, Yantong Zhou; Investigation: Tianyu Zhu; Visualization: Ruihong Yu; Supervision: Zheng Wang; Formal analysis: Yawei Qiu, Zhangshun; Data curation: Jinfeng Miao; Funding acquisition: Zhenguang Liu; Writing—original draft: Deyun Wang, Lina Jiao; Writing—review & editing: Lina Jiao, Zhenguang Liu;

Declaration of competing interest

The authors declare that they have no known competing financial interests or personal relationships that could have appeared to influence the work reported in this paper.

Acknowledgments

The author thanks all other staff members of the Institute of Traditional Chinese Medicine and Veterinary Medicine at Nanjing Agricultural University for their assistance in this study.

References

Amanna, I.J., Slifka, M.K., 2010. Mechanisms that determine plasma cell lifespan and the duration of humoral immunity. Immunol. Rev. 236, 125–138.
Angelin-Duclos, C., Cattoretti, G., Lin, K.-I., Calame, K., 2000. Commitment of B lymphocytes to a plasma cell fate is associated with blimp-1 expression In Vivo1. J. Immunol. 165, 5462–5471.
Ansel, K.M., Djuretic, I.., Tanasa, B., Rao, A., 2006. Regulation of Th2 differentiation and Il4 locus accessibility. Annu. Rev. Immunol. 24, 607–656.
Arsenio, J., 2020. Single-cell analysis of CD8 T lymphocyte diversity during adaptive immunity. WIREs. Syst. Biol. Med. 12, e1475.
Ashby, K.M., Hogquist, K.A., 2024. A guide to thymic selection of T cells. Nat. Rev. Immunol. 24, 103–117.
Bernstein, D.I., Edwards, K..M., Dekker, C.L., Belshe, R., Talbot, H.K.B., Graham, I.L., Noah, D.L., He, F., Hill, H., 2008. Effects of adjuvants on the safety and immunogenicity of an Avian Influenza H5N1 vaccine in adults. J. Infect. Dis. 197, 667–675.
Bhagchandani, S. H., .L.. Yang, J. H. Lam, L. Maiorino, E. Ben-Akiva, K. A. Rodrigues, A. Romanov, H. Suh, A. Aung, S. Wu, A. Wadhera, A. K. Chakraborty, and D. J. Irvine. Two-dose priming immunization amplifies humoral immunity by synchronizing vaccine delivery with the germinal center response. Sci. Immunol. 9:eadl3755.
Bin Aslam, H., Häsler, B., Iqbal, M., Yaqub, T., Alarcon, P., 2024. Financial impact of low pathogenic avian influenza virus subtype H9N2 on commercial broiler chicken and egg layer production systems in Pakistan. Prevent. Vet. Med. 233, 106346.
Bollig, N., Brüstle, A., Kellner, K., Ackermann, W., Abass, E., Raifer, H., Camara, B., Brendel, C., Giel, G., Bothur, E., Huber, M., Paul, C., Elli, A., Kroczek, R.A., Nurieva, R., Dong, C., Jacob, R., Mak, T.W., Lohoff, M., 2012. Transcription factor IRF4 determines germinal center formation through follicular T-helper cell differentiation. Proc. Natl. Acad. Sci. USA. 109, 8664–8669.
Bonfante, F., Mazzetto, E., Zanardello, C., Fortin, A., Gobbo, F., Maniero, S., Bigolaro, M., Davidson, I., Haddas, R., Cattoli, G., Terregino, C., 2018. A G1-lineage H9N2 virus with oviduct tropism causes chronic pathological changes in the infundibulum and a long-lasting drop in egg production. Vet. Res. 49, 83.
Borland, S., P. Gracieux, M. Jones, F. Mallet, and J. Yugueros-Marcos. 2020. Influenza A virus infection in cats and dogs: a literature review in the light of the "one health" concept. Front. Public health. 8:83.
Camilloni, B., Basileo, M., Valente, S., Nunzi, E., Iorio, A.M., 2015. Immunogenicity of intramuscular MF59-adjuvanted and intradermal administered influenza enhanced vaccines in subjects aged over 60: a literature review. Hum. Vaccin. Immunother. 11, 553–563.
Cancro, M.P., Tomayko, M.M., 2021. Memory B cells and plasma cells: the differentiative continuum of humoral immunity. Immunol. Rev. 303, 72–82.
Castro-Sanguinetti, G.R., González-Veliz, R.., Callupe-Leyva, A., Apaza-Chiara, A.P., Jara, J., Silva, W., Icochea, E., More-Bayona, J.A., 2024. Highly pathogenic avian influenza virus H5N1 clade 2.3.4.4b from Peru forms a monophyletic group with Chilean isolates in South. America. Sci. Rep. 14, 3635.
Choi, E.-h., Song, M.-S., Park, S.-J., Pascua, P.N.Q., Baek, Y.H., Kwon, H.-i., Kim, E.-H., Kim, S., Jang, H.-K., Poo, H., Kim, C.-J., Choi, Y.K., 2015. Development of a dual-protective live attenuated vaccine against H5N1 and H9N2 avian influenza viruses by modifying the NS1 gene. Arch. Virol. 160, 1729–1740.
Comerford, I., Harata-Lee, Y., Bunting, M.D., Gregor, C., Kara, E.E., McColl, S.R., 2013. A myriad of functions and complex regulation of the CCR7/CCL19/CCL21 chemokine axis in the adaptive immune system. Cytokine & Growth Factor Rev 24, 269–283.
Cui, A., Huang, T., Li, S., Ma, A., Pérez, J.L., Sander, C., Keskin, D.B., Wu, C.J., Fraenkel, E., Hacohen, N., 2024. Dictionary of immune responses to cytokines at single-cell resolution. Nature 625, 377–384.
Dharmayanti, N., Indriani, R., Nurjanah, D., 2020. Vaccine efficacy on the novel reassortant H9N2 virus in Indonesia. Vaccines (Basel) 8.
Dong, J., Zhou, Y., Pu, J., Liu, L., 2022. Status and challenges for vaccination against Avian H9N2 influenza virus in China. Life (Basel) 12.
Feltelius, N., Persson, I., Ahlqvist-Rastad, J., Andersson, M., Arnheim-Dahlström, L., Bergman, P., Granath, F., Adori, C., Hökfelt, T., Kühlmann-Berenzon, S., Liljeström, P., Maeurer, M., Olsson, T., Örtqvist, Å., Partinen, M., Salmonson, T., Zethelius, B., 2015. A coordinated cross-disciplinary research initiative to address an increased incidence of narcolepsy following the 2009-2010 Pandemrix vaccination programme in Sweden. J. Intern. Med. 278, 335–353.
Gu, M., Xu, L., Wang, X., Liu, X., 2017. Current situation of H9N2 subtype avian influenza in China. Vet. Res. 48.
Guo, B., Fu, S., Zhang, J., Liu, B., Li, Z., 2016. Targeting inflammasome/IL-1 pathways for cancer immunotherapy. Sci. Rep. 6, 36107.
Guo, X., Liao, M., Xin, C., 2003. Sequence of HA gene of Avian Influenza A/Chicken/Guangdong/SS/1994 (H9N2) virus. Avian Dis. 47, 1118–1121.
Heeringa, M., Leav, B., Smolenov, I., Palladino, G., Isakov, L., Matassa, V., 2020. Comparability of titers of antibodies against seasonal Influenza virus strains as determined by hemagglutination inhibition and microneutralization assays. J. Clin. Microbiol. 58. https://doi.org/10.1128/jcm.00750-00720.
Hivroz, C., Saitakis, M., 2016. Biophysical aspects of T lymphocyte activation at the immune synapse. Front Immunol. 7, 46.
Hu, G., Zhao, K., 2016. Looping around Bcl6 in Germinal Center to Sharpen B. Cell Immun. Immun. 45, 459–461.
Jia, F., Wang, W., Tian, Y., Zahra, A., He, Y., Ge, C., Zhang, T., Wang, M., Gong, J., Zhang, G., Yang, G., Yang, W., Shi, C., Wang, J., Huang, H., Cao, X., Zeng, Y., Wang, N., Wang, Z., Wang, C., Jiang, Y., 2025. Delivery of dendritic cells targeting 3M2e-HA2 nanoparticles with a CpG adjuvant via lysosomal escape of Salmonella enhances protection against H9N2 avian influenza virus. Poultry. Sci. 104, 104616.
Jiang, P., Zhang, Y., Ru, B., Yang, Y., Vu, T., Paul, R., Mirza, A., Altan-Bonnet, G., Liu, L., Ruppin, E., Wakefield, L., Wucherpfennig, K.W., 2021. Systematic investigation of cytokine signaling activity at the tissue and single-cell levels. Nat. Methods. 18, 1181–1191.
Jin, Z., Liu, J., Guo, S., Xu, S., Gong, X., Zhang, C., Zhao, K., 2025. N-2-hydroxypropyl trimethyl ammonium chloride chitosan-aluminum nano-adjuvant elicit strong

immune responses in porcine epidemic diarrhea inactivated vaccine. Int. J. Nanomedicine 20, 1321–1334.
Ko, K.H., Lee, I..K., Kim, G., Gu, M.J., Kim, H.Y., Park, B.-C., Park, T.S., Han, S.H., Yun, C.-H., 2018. Changes in bursal B cells in chicken during embryonic development and early life after hatching. Sci. Rep. 8, 16905.
Lai, Y., Wang, S., Shen, X., Qi, R., Liu, T., Du, F., YuHe, Y., Miao, B., Zhai, J., Zhang, Y., Liu, S., Chen, Z., 2025. An injectable chitosan hydrochloride-sodium alginate hydrogel adjuvant capable of eliciting potent humoral and cellular immunity. ACS Appl. Mater. Interfaces. 17, 14444–14459.
Lewis, S.M., Williams, A.., Eisenbarth, S.C., 2019. Structure and function of the immune system in the spleen. Sci. Immunol 4, eaau6085.
Li, X., Ju, H., Liu, J., Yang, D., Qi, X., Yang, X., Qiu, Y., Zheng, J., Ge, F., Zhou, J., 2017. Influenza virus-like particles harboring H9N2 HA and NA proteins induce a protective immune response in chicken. Influenza Other Respiratory Viruses 11, 518–524.
Li, X., Shi, J., Guo, J., Deng, G., Zhang, Q., Wang, J., He, X., Wang, K., Chen, J., Li, Y., Fan, J., Kong, H., Gu, C., Guan, Y., Suzuki, Y., Kawaoka, Y., Liu, L., Jiang, Y., Tian, G., Li, Y., Bu, Z., Chen, H., 2014. Genetics, receptor binding property, and transmissibility in mammals of naturally isolated H9N2 Avian Influenza viruses. PLoS. Pathog. 10, e1004508.
Li, X., Xie, Z., Wei, Y., Li, M., Zhang, M., Luo, S., Xie, L., 2024. Recombinant hemagglutinin protein from H9N2 Avian Influenza Virus exerts good immune effects in mice in microorganisms. Microorganisms. 12 (8), 1552.
Liu, J., Guo, S., Jin, Z., Zhao, K., 2023a. Adjuvanted quaternized chitosan composite aluminum nanoparticles-based vaccine formulation promotes immune responses in chickens. Vaccine 41, 2982–2989.
Liu, Y., Chen, Y., Yang, Z., Lin, Y., Fu, S., Chen, J., Xu, L., Liu, T., Niu, B., Huang, Q., Liu, H., Zheng, C., Liao, M., Jia, W., 2024a. Evolution and antigenic differentiation of Avian Influenza A(H7N9) Virus, China. Emerg. Infect. Dis. 30, 1218–1222.
Liu, Y., Yu, Q., Zhou, X., Li, W., He, X., Wang, Y., Deng, G., Shi, J., Tian, G., Zeng, X., Chen, H., 2024b. Inactivated H9N2 vaccines developed with early strains do not protect against recent H9N2 viruses: call for a change in H9N2 control policy. J. Integr. Agric. 23, 2144–2148.
Liu, Y., Zhao, D., Zhang, J., Huang, X., Han, K., Liu, Q., Yang, J., Zhang, L., Li, Y., 2023b. Development of an inactivated Avian Influenza Virus vaccine against circulating H9N2 in chickens and ducks. Vaccines. (Basel) 11.
Luo, W., Weisel, F., Shlomchik, M.J., 2018. B cell receptor and CD40 signaling are rewired for synergistic induction of the c-myc transcription factor in germinal center B cells. Immunity 48, 313–326.e315.
Marrack, P., McKee, A.S., Munks, M.W., 2009. Towards an understanding of the adjuvant action of aluminium. Nat. Rev. Immunol. 9, 287–293.
Moore, K.W., de Waal Malefyt, R.., Coffman, R.L., O'Garra, A., 2001. Interleukin-10 and the interleukin-10 receptor. Annu. Rev. Immunol. 19, 683–765.
Morimoto, R., Matsubara, C., Hanada, A., Omoe, Y., Ogata, T., Isegawa, Y., 2022. Effect of structural differences in naringenin, prenylated naringenin, and their derivatives on the Anti-Influenza Virus activity and cellular uptake of their flavanones. Pharmaceuticals (Basel) 15 (12), 1480.
Mujal, A.M., Owyong, M.., Santosa, E.K., Sauter, J.C., Grassmann, S., Pedde, A.-M., Meiser, P., Wingert, C.K., Pujol, M., Buchholz, V.R., Lau, C.M., Böttcher, J.P., Sun, J. C., 2025. Splenic TNF-α signaling potentiates the innate-to-adaptive transition of antiviral NK cells. Immunity 58, 585–600.e586.
Ninfali, P., Antonelli, A., Magnani, M., Scarpa, E.S., 2020. Antiviral properties of flavonoids and delivery strategies. Nutrients. 12 (9), 2534.
Ochiai, K., Maienschein-Cline, M., Simonetti, G., Chen, J., Rosenthal, R., Brink, R., Chong, A.n.S., Klein, U., Dinner, A.a.R., Singh, H., Sciammas, R., 2013. Transcriptional regulation of germinal center B and plasma cell fates by dynamical control of IRF4. Immunity 38, 918–929.
Pan, X., Liu, Q., de Jong, M.C.M., Forlenza, M., Niu, S., Yan, D., Teng, Q., Li, X., Beerens, N., Li, Z., 2023. Immunoadjuvant efficacy of CpG plasmids for H9N2 avian influenza inactivated vaccine in chickens with maternal antibodies. Vet. Immunol. Immunopathol. 259, 110590.
Pereira, M.V.A., Galvani, R.G., Gonçalves-Silva, T., de Vasconcelo, Z.F.M., Bonomo, A., 2024. Tissue adaptation of CD4 T lymphocytes in homeostasis and cancer. Front Immunol 15, 1379376.
Qian, C., Liu, X., Xu, Q., Wang, Z., Chen, J., Li, T., Zheng, Q., Yu, H., Gu, Y., Li, S., Xia, N., 2020. Recent progress on the versatility of virus-like particles. Vaccines (Basel) 8.
Rau, F.C., Dieter, J.., Luo, Z., Priest, S.O., Baumgarth, N., 2009. B7-1/2 (CD80/CD86) Direct signaling to B cells enhances IgG Secretion1. J. Immunol. 183, 7661–7671.
Rehman, M.U., Rahman Mir, M..U., Farooq, A., Rashid, S.M., Ahmad, B., Bilal Ahmad, S., Ali, R., Hussain, I., Masoodi, M., Muzamil, S., Madkhali, H., Ahmad Ganaie, M., 2018. Naringenin (4,5,7-trihydroxyflavanone) suppresses the development of precancerous lesions via controlling hyperproliferation and inflammation in the colon of Wistar rats. Environ. Toxicol. 33, 422–435.
Roubidoux, E.K., Carreño, J..M., McMahon, M., Jiang, K., van Bakel, H., Wilson, P., Krammer, F., 2021. Mutations in the hemagglutinin stalk domain do not permit escape from a protective, stalk-based vaccine-induced immune response in the mouse model. mBio 12 (1), e03617–e03620.
Sagong, M., Lee, K.-N., Lee, E.-K., Kang, H., Choi, Y.K., Lee, Y.-J., 2023. Current situation and control strategies of H9N2 avian influenza in South Korea. J. Vet. Sci. 24 (1), e5.
Santosa, E.K., Sun, J.C., 2023. Cardinal features of immune memory in innate lymphocytes. Nat. Immunol. 24, 1803–1812.
Saxton, R.A., Tsutsumi, N.., Su, L.L., Abhiraman, G.C., Mohan, K., Henneberg, L.T., Aduri, N.G., Gati, C., Garcia, K.C., 2021. Structure-based decoupling of the pro- and anti-inflammatory functions of interleukin-10. Science 371.
Seyed, N., Rafati, S., 2021. Th1 concomitant immune response mediated by IFN-γ protects against sand fly delivered Leishmania infection: implications for vaccine design. Cytokine 147, 155247.
Shehata, L., Thouvenel, C.D., Hondowicz, B.D., Pew, L.A., Pritchard, G.H., Rawlings, D. J., Choi, J., Pepper, M., 2024. Interleukin-4 downregulates transcription factor BCL6 to promote memory B cell selection in germinal centers. Immunity 57, 843–858. e845.
Shichinohe, S., Watanabe, T., 2023. Advances in adjuvanted influenza vaccines. Vaccines (Basel) 11 (8), 1391.
Shin, J.-H., Mo, J.S., Kim, J.-N., Mo, I.-p., Ha, B.-D., 2016. Assessment of the safety and efficacy of low pathogenic avian influenza (H9N2) virus in inactivated oil emulsion vaccine in laying hens. J. Vet. Sci. 17, 27–34.
Singh, S., Sharma, A., Monga, V., Bhatia, R., 2023. Compendium of naringenin: potential sources, analytical aspects, chemistry, nutraceutical potentials and pharmacological profile. Crit. Rev. Food Sci. Nutr. 63, 8868–8899.
Sturkenboom, M.C., 2015. The narcolepsy-pandemic influenza story: can the truth ever be unraveled? Vaccine 33 Suppl 2, B6–b13.
Subbarao, K., 2021. Live attenuated cold-adapted influenza vaccines. Cold Spring Harb Perspect Med 11 (9), a038653.
Sun, L., Zhao, X., Liu, X., Zhong, B., Tang, H., Jin, W., Clevers, H., Wang, H., Wang, X., Dong, C., 2021. Transcription factor Ascl2 promotes germinal center B cell responses by directly regulating AID transcription. Cell Rep 35, 109188.
Sun, Y., Liu, J., 2015. H9N2 influenza virus in China: a cause of concern. Protein & Cell 6, 18–25.
Sun, Y., Pu, J., Fan, L., Sun, H., Wang, J., Zhang, Y., Liu, L., Liu, J., 2012. Evaluation of the protective efficacy of a commercial vaccine against different antigenic groups of H9N2 influenza viruses in chickens. Vet. Microbiol. 156, 193–199.
Sun, Y., Pu, J., Jiang, Z., Guan, T., Xia, Y., Xu, Q., Liu, L., Ma, B., Tian, F., Brown, E.G., Liu, J., 2010. Genotypic evolution and antigenic drift of H9N2 influenza viruses in China from 1994 to 2008. Vet. Microbiol. 146, 215–225.
Tan, M., Zeng, X., Xie, Y., Li, X., Liu, J., Yang, J., Yang, L., Wang, D., 2023. Reported human infections of H9N2 avian influenza virus in China in 2021. Front Public Health 11, 1255969.
Tregoning, J.S., Russell, R..F., Kinnear, E., 2018. Adjuvanted influenza vaccines. Hum. Vaccin. Immunother. 14, 550–564.
Trevejo, J.M., Marino, M..W., Philpott, N., Josien, R., Richards, E.C., Elkon, K.B., Falck-Pedersen, E., 2001. TNF-α-dependent maturation of local dendritic cells is critical for activating the adaptive immune response to virus infection. Proc. Natl. Acad. Sci. 98, 12162–12167.
Viant, C., Weymar, G.H.J., Escolano, A., Chen, S., Hartweger, H., Cipolla, M., Gazumyan, A., Nussenzweig, M.C., 2020. Antibody affinity shapes the choice between memory and germinal center B cell fates. Cell. 183, 1298–1311.e1211.
Wang, M., Wei, Y., Pu, J., Bing, G., Sun, Y., Sun, H., Wei, F., Liu, J., 2018. Cross-immunity of a H9N2 live attenuated influenza vaccine against H5N2 highly pathogenic avian influenza virus in chickens. Vet. Microbiol. 220, 57–66.
Watanabe, M., Fujihara, C., Radtke, A.J., Chiang, Y.J., Bhatia, S., Germain, R.N., Hodes, R.J., 2017. Co-stimulatory function in primary germinal center responses: CD40 and B7 are required on distinct antigen-presenting cells. J. Exp. Med. 214, 2795–2810.
Wu, Q., Wang, W., Zhang, X., Li, D., Mei, M., 2024. Effectively evaluating a novel consensus subunit vaccine candidate to prevent the H9N2 Avian influenza virus. Vaccines (Basel). 12 (8), 849.
Xie, Z., Chen, Y., Xie, J., Du, S., Chen, R., Zheng, Y., You, B., Feng, M., Liao, M., Dai, M., 2025. Construction with recombinant epitope-expressing baculovirus enhances protective effects of inactivated H9N2 vaccine against heterologous virus. Vet. Microbiol. 300, 110337.
Xu, C., Fan, W., Wei, R., Zhao, H., 2004. Isolation and identification of swine influenza recombinant A/Swine/Shandong/1/2003(H9N2) virus. Microbes Infect 6, 919–925.
Xu, S., Yu, L., Teng, Q., Li, X., Jin, Z., Qu, Y., Li, J., Zhang, Q., Li, Z., Zhao, K., 2023. Enhance immune response to H9 AIV DNA vaccine based on polygene expression and DGL nanoparticle encapsulation. Poult. Sci. 102, 102925.
Xu, X., Qian, J., Qin, L., Li, J., Xue, C., Ding, J., Wang, W., Ding, W., Yin, R., Jin, N., Ding, Z., 2020. Chimeric Newcastle disease virus-like particles containing DC-binding peptide-fused haemagglutinin protect chickens from virulent Newcastle Disease virus and H9N2 Avian Influenza Virus challenge. Virol. Sin. 35, 455–467.
Xue, R., Tian, Y., Hou, T., Bao, D., Chen, H., Teng, Q., Yang, J., Li, X., Wang, G., Li, Z., Liu, Q., 2018. H9N2 influenza virus isolated from minks has enhanced virulence in mice. Transbound. Emerg. Dis. 65, 904–910.
Yan, S., Chen, Y., Lin, J., Chen, H., Hu, C., Liu, H., Diao, H., Liu, S., Chen, J.-L., 2024. Recombinant avian-derived antiviral proteins cIFITM1, cIFITM3, and cViperin as effective adjuvants in inactivated H9N2 subtype avian influenza vaccines. Vet. Microbiol. 298, 110277.
Yang, W.-T., Yang, G.-L., Shi, S.-H., Liu, Y.-Y., Huang, H.-B., Jiang, Y.-L., Wang, J.-Z., Shi, C.-W., Jing, Y.-B., Wang, C.-F., 2017. Protection of chickens against H9N2 avian influenza virus challenge with recombinant Lactobacillus plantarum expressing conserved antigens. Appl. Microbiol. Biotechnol. 101, 4593–4603.
Yang, W., Liu, X., Wang, X., 2023. The immune system of chicken and its response to H9N2 avian influenza virus. Vet. Q. 43, 1–14.
Yong-feng, Z., Fei-fei, D., Jia-yu, Y., Feng-xia, Z., Chang-qing, J., Jian-li, W., Shou-yu, G., Kai, C., Chuan-yi, L., Xue-hua, W., Jiang, S.-j., Zhi-jing, X., 2017. Intraspecies and interspecies transmission of mink H9N2 influenza virus. Sci. Rep 7, 7429.
Yu, H., Hua, R.-H., Wei, T.-C., Zhou, Y.-J., Tian, Z.-J., Li, G.-X., Liu, T.-Q., Tong, G.-Z., 2008. Isolation and genetic characterization of avian origin H9N2 influenza viruses from pigs in China. Vet. Microbiol. 131, 82–92.
Zeng, X., Li, J., Liu, J., Mo, L., Liu, Y., Zhang, A., Yang, P., Kong, H., 2024. Nasal mucosal fibroblasts produce IL-4 to induce Th2 response. Innate. Immun 30, 55–65.

Zhang, H., Xie, R., Zhang, H., Sun, R., Li, S., Xia, C., Li, Z., Zhang, L., Guo, Y., Huang, J., 2023. Recombinant hemagglutinin protein and DNA-RNA-combined nucleic acid vaccines harbored by yeast elicit protective immunity against H9N2 avian influenza infection. Poult. Sci. 102, 102662.
Zhang, K., Zhang, Z., Yu, Z., Li, L., Cheng, K., Wang, T., Huang, G., Yang, S., Zhao, Y., Feng, N., Fu, J., Qin, C., Gao, Y., Xia, X., 2013. Domestic cats and dogs are susceptible to H9N2 avian influenza virus. Virus Res. 175, 52–57.
Zhang, T., Tian, Y., Zhang, X., Wang, W., He, Y., Ge, C., Jia, F., Wang, Z., Jiang, Y., 2024. Improved cellular immune response induced by intranasal boost immunization with chitosan coated DNA vaccine against H9N2 influenza virus challenge. Microb. Pathog. 195, 106871.
Zhao, J., Zhang, Y., Zhao, Q., He, Y., Li, Z., Chen, A., Wang, C., Wang, B., Jiao, B., Cui, Y., 2021. A sensitive and practical ELISA for analyzing naringenin in pummelo and herb samples. Food Chem 362, 130223.
Zhou, P., Qiu, T., Wang, X., Yang, X., Shi, H., Zhu, C., Dai, W., Xing, M., Zhang, X., Xu, J., Zhou, D., 2024. One HA stalk topping multiple heads as a novel influenza vaccine. Emerg. Microbes. Infect. 13, 2290838.
Zhu, R., Xu, S., Sun, W., Li, Q., Wang, S., Shi, H., Liu, X., 2022. HA gene amino acid mutations contribute to antigenic variation and immune escape of H9N2 influenza virus. Vet. Res. 53, 43.